CHALLENGE JOURNAL OF CONCRETE RESEARCH LETTERS 8 (3) (2017) 70–83

Feasibility of using self-compacting concrete in civil engineering applications

Mounir M. Kamal [a], Zeinab A. Etman [a,*], Mohamed R. Afify [a], Tamer I. Ahmed [b]

[a] *Department of Civil Engineering, Menoufia University, Shebin ElKoum, Menofia, Egypt*
[b] *Department of Civil Engineering, Higher Institute of Engineering and Technology, Kafr el-Sheikh, Egypt*

ABSTRACT

This research aimed to investigate the feasibility of using self-compacting concrete in civil engineering applications as a producing a precast hollow unit. The behavior of the hollow sections cast with self-compacted concrete beneath line-load was evaluated. An experimental work was carried out and a finite element model with ANSYS (version 15) was adopted. A total of fourteen hollow beams were cast and tested. The most variables taken into thought were; the types of reinforcement (reinforced steel bar and steel wire meshes), the types of steel wire meshes (expanded and welded steel wire mesh), number of layers of steel meshes (one layer and two layers), cross section thickness of concrete (40 mm and 60mm), concrete cover thickness (15mm and 20 mm) and also the shapes of cross section (square or circular). Special attention to initial cracking load, ultimate load, deflection, cracking pattern, energy absorption and ductility index were investigated. Good agreement was found compared with the experimental results. Out of this research; this paper presents applications of self-compacted concrete for casting skinny structural hollow members. These members can be used as precast units within the construction of the tunnel to decrease the problems in highway roads due to the difficulty of using crossing bridges particularly for kids and old people which are very useful for developing countries with great economic advantages.

ARTICLE INFO

Article history:
Received 26 June 2017
Revised 1 September 2017
Accepted 6 September 2017

Keywords:
Self-compacting concrete
Wire mesh
Thin hollow beams
Ductility index
Energy absorption
Economic assessment

1. Introduction

Self–compacting concrete (SCC) is new particular concrete recommended for all several applications particularly in extremely reinforced concrete members like bridge decks or abutments tunnel linings tubing segments, wherever it is difficult to vibrate the concrete, dames, underground structures, composite structures, or may be for traditional engineering structures (Klug and Holschemacher, 2003). There are several factors effects on the workability of self-compacted concrete like the sort of construction, the chosen placement and consolidation methods, the shape of the form-work and also the nature of the reinforcement (Khayat et al., 1997). The absence of the vibration is decreasing the pressure; the modified consistency dose will increase the loads (Abdel Hady, 2003). To create SCC fascinating for the application especially as a prepared ready mix concrete, the value of the manufacturing SCC compared to traditional concrete should be reduced (Proske and Graubner, 2002). The characteristic of SCC to flow free segregation into formwork without the requirement for vibration affects absolutely the distribution of the concrete strength even in massive concrete members (Khayat et al., 1997; Vanhove et al., 2001). Pereira-de-Oliveira et al. (2013) studied the porousness of SCC with recycled aggregate incorporation. Sara et al. (2017) presented a literature review on the behavior of self-compacting concrete at fresh state with fine and coarse recycled aggregates. They concluded that SCC with recycled aggregates is of great relevance to society that rationalized the negative effects on the atmosphere. Olga et al. (2016) were

* *Corresponding author*. Tel.: +2-01-009-727355 ; E-mail address: zeinab.etman@sh-eng.menofia.edu.eg (Z. A. Etman)
ISSN: 2548-0928 / DOI: https://doi.org/10.20528/cjcrl.2017.03.001

carried out an experimental program on SCC-type mixtures pump ability to spot the most parameters for pumping quality control. Results discovered that also when the cast in situ procedure is correctly performed; it will have an effect on each the early age performance and also the hardened properties of the SCC-type mixtures. Habib et al. (2016) evaluated the performance of various self-consolidating concrete (SCC) mixtures in a full-scale reinforced concrete beams. The result of combine of mix design and the stability of the SCC on the flowability and passing ability of the concrete cast within the vertical and horizontal directions along the beams are evaluated. The first application of SCC was during a building in June 1990, and so it absolutely was employed in several applications like the towers of a pre-stressed cable-stayed bridge in 1991. In 1992, a special type of lightweight SCC was used in the main girder of a cable-stayed bridge. Since then the utilization of SCC in actual structures has bit by bit increased with the aim that SCC are going to be the normal form of concrete. SCC is applied in precast plants, wherever special conditions are available (Skarendahi, 1998). A typical application of SCC is that the two anchorages of Akashi–Kaikyo Bridge opened in April 1998 a suspension bridge with the longest span in the world (1,991meters). A new construction system that makes full use of the performance of SCC, the concrete was mixed at the lot of batch plant beside the site and was the pumped out of the plant. The utilization of SCC shortened the anchorage construction period by 20% from 2.5 to 2 years (Ouchi, 2000). Manikandanet et al. (2015) presented the flexural behavior of hollow core sandwich beams with completely different core shape, by using expanded polystyrene foam within the tension zone of beams. The results showed associate improvement within the behavior of hollow core sandwich beams compared with conventional solid beams. Djamaluddin et al. (2014) conducted an experimental study on fully removed concrete in the tensile zone. They studied the effect of removed concrete on the flexural mechanical action between tension stress and compression stress of the concrete beam section because the flexural capacity of the beam decreases. Kocher et al. (2002) presented a theoretical study of sandwich structures with polymer frame reinforced with hollow core using simple analytical models that describe the contribution to the stability of the structure in hollow at the core. Shirai and Ohama (1990) used polymer-modified mortar rather than ordinary cement mortar to improve the flexural behavior and impact resistance of ferrocement. Yogendran (1987) studied the effect of silica fume in the properties of high-strength concrete. He concluded that the optimum percentage of silica 15% as a replacement of cement content at the water-cement ratio of 0.34.

2. Research Significance

This paper introduces a new effective and economic technique for constructing tunnel using permanent precast units casting with SCC. The objectives of the experimental program described within this research were (i) studying the behavior of reinforced thin hollow beams cast with SCC under line-load as in Fig. (1). (ii) Studying the effect of the type of reinforcement, type and number of layers of steel wire meshes, the shape of the cross section, thickness of concrete cover and cross-sectional. (iii) Evaluating the economic assessment of thin hollow sections as precast tunnel units. Theoretical analysis will be conducted by ANSYS 15 as a finite element package to verify the results of the experimental program.

3. Experimental Program

To evaluate the aim of this study, fourteen reinforced hollow beams were conducted. 1500 mm in length is for the tested sections. A square cross section has a dimension 400 mm×400 mm. A circular cross section has a diameter 400 mm. 60 mm and 40 mm were the cross-sectional thickness for reinforced by steel bars and steel wire meshes, respectively. The geometrical and reinforcement details of the tested beams are shown in Table 1 and Fig. 1. Fig. 2 shows the test set-up. The test specimens were painted with white paint to clarify the visual cracks during the testing. To measure the deflection, demec points were placed during loading. I beam 15 with 2 m in length was used for line load. The subsequent code was used for the sample designation: the first letter defines shaped cross section (Q for the square cross section and C for the circular cross section) the second letter S defines the steel reinforcement. The letter W is for welded steel wire mesh. The letter (ex) is for expanded wire mesh. Letter V defines the cover concrete which is equal 15 mm. The letter r defines the stirrups used with the steel wire mesh. The number 1 is for one layer steel wire mesh also the number 2 is for two layers steel wire mesh.

4. Material Properties

Ordinary Portland cement type I (CEMI 42.5N) according to the requirements of E.S.S. 4756-11, 2009 with a specific gravity of 3.15 and a specific surface area (Blaine fineness) 3700 cm^2/gm. was used. Locally produced identified Silica Fume (S.F.) was delivered in 25-Kg sacks according to the manufacturer; the powder had an average particle size of 0.1 micrometers, specific surface area 170000 cm2/gm. and specific gravity of 2.2. Natural siliceous sand was used as fine aggregate throughout the current research. The fine aggregates used was obtained from Suez zone with 2.62 specific gravity, 2.67 fineness modulus and absorption percentage of 0.79%. Coarse aggregate (dolomite) with a nominal size of 10 mm was used; with a specific gravity 2.64 and absorption value of 1.8%. Viscocrete 5930 L as high range water reducer (HRWR) complies with ASTM C494 Type A & F was used. Expanded metal wire mesh and welded steel wire mesh were used as reinforcement. The geometric properties of these mashes accommodates of ACI 549.1R-97, as shown in Fig. 3 and Table 2. Tensile tests on welded steel wire mesh and expanded metal wire mesh were carried out. The proof stress for welded steel wire meshes and expanded metal wire meshes were 315 and 210 N/mm^2, respectively. The ultimate

tensile strength for welded steel wire meshes and expanded metal wire meshes were 600 and 315 N/mm^2, respectively. Mild steel rebar (nominal diameters 8 mm) was used as main reinforcement with yield and ultimate tensile strength of 292 and 455 N/mm^2, respectively. Mild steel rebar was used for stirrups (nominal diameters 6 mm) with yield and ultimate tensile strength of 254 and 390 N/mm^2, respectively.

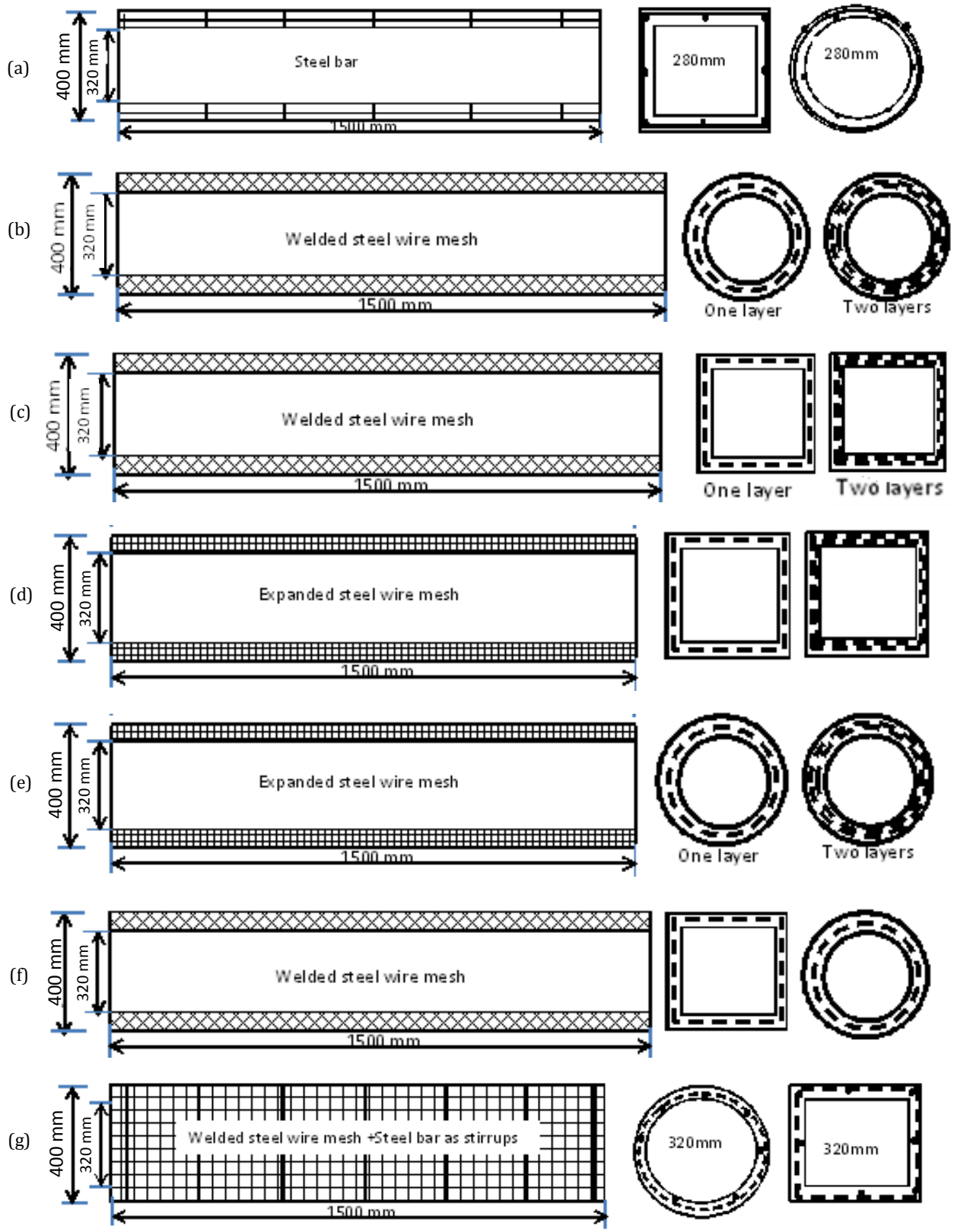

Fig. 1. Geometrical and reinforcement details of the tested hollow beams: (a) QS and CS; (b) C1W and C2W; (c) Q1W and Q2W; (d) Q1ex and Q2ex; (e) C1ex and C2ex; (f) Q1wv and C1wv; (g) Q1wr and C1wr.

Table 1. Details of the tested specimens.

Designation of Beam	Reinforcing Wire Mesh			Steel Reinforcement		Thickness (mm)	Length (mm)	Concrete cover (mm)	Total weight of steel (kg)
	Type	No. of layers	V_f*%	Longitudinal	Stirrups				
QS	-	-	-	Φ 8/ 15 cm	ϕ6/20 cm	60	1500	20	6
CS	-	-	-	Φ 8/ 15 cm	ϕ6/20 cm				5.8
Q1w	welded	1	5.2	-	-	40			1.2
C1w	mesh	1	5.4	-	-				1.15
Q1ex	expanded	1	6.3	-	-				1.25
C1ex	mesh	1	6.5	-	-				1.2
Q2w	welded	2	10.4	-	-				2.4
C2w	mesh	2	10.8	-	-				2.3
Q2ex	expanded	2	12.6	-	-				2.5
C2ex	mesh	2	13	-	-				2.4
Q1wv		1	5.2	-	-			15	1.2
C1wv	welded	1	5.4	-	-				1.15
Q1wr	mesh	1	10.2	-	ϕ6/20 cm			20	2.97
C1wr		1	10.4	-	ϕ6/20 cm				2.92

* V_f: Volume fraction of wire mesh

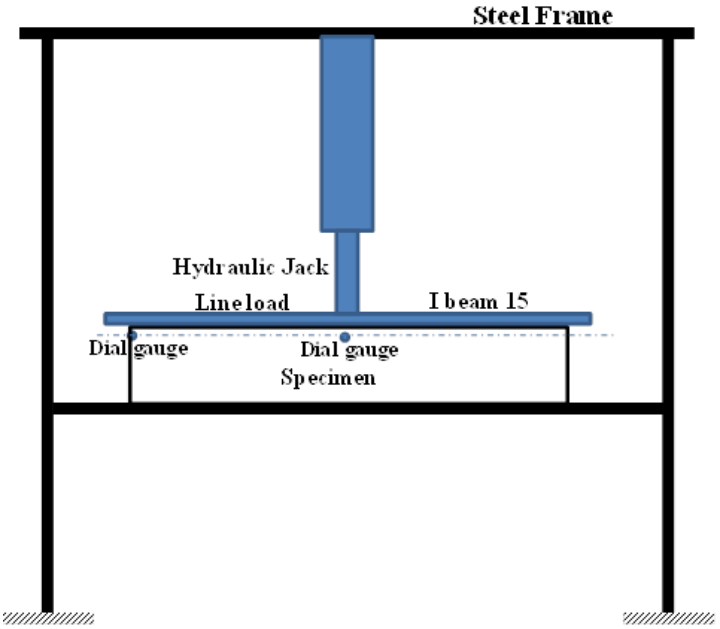

Fig. 2. Test set-up.

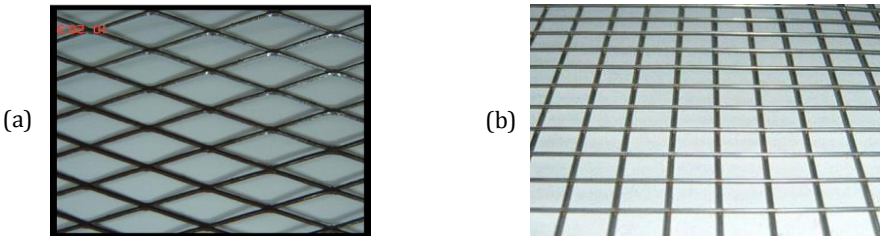

Fig. 3. Types of steel mesh: (a) Expanded steel wire mesh; (b) Welded steel wire mesh.

Table 2. Geometric properties of the steel meshes.

Mesh Type	Mesh Opening (mm)		Dimension of Strands (mm)	Diameter (mm)		Grid Size (mm)	Weight (kg/m²)
	Long Way	Short Way		Width	Thickness		
Square welded wire fabric	25	25	1.2	0.7	1.4	25x25	2.5
Expanded (metal) mesh	12.7	12.7	2.40	1.25	1.25	12.7x12.7	3

5. Casting and Testing Procedures

Square specimens placed into molds with the longitudinal axis being vertical. Concrete was poured gently in one layer up to the highest edge, minimizing entrapped air wherever the smoothness of the formed surfaces is important, the concrete spaded along the molds or gently tapped on the perimeters of the molds with a mallet. Molds maintained vertical throughout and once inserting till concrete hardens. For circular specimens, centrifugal force casting (rotating machine) with the same mix design was used (Table 3). The specimens were kept in molds for three days once casting and expose to 100ºC. Afterward that the specimens were immerged in clean water till taken out for testing.

Table 3. Mix proportions (kg/m^3).

Cement	Sand	Dolomite	VEA	S.F.	Water	F_{cu} (N/mm^2), 28 days
400	1036	850	8	20	140	44

VEA: ViscoCrete-5930 L S.F.: Silica fume F_{cu}: compressive strength

6. Results and Discussion

6.1. Effect of shape of cross section

Fig. 4 shows the effect of the shape of the cross-section for the tested beam with different types of reinforcement. It is noticed that the loads for the beams with square cross sections was higher than that of circular cross sectional. This due to value of the moment of inertia of square section is bigger than the circular section. Fig.4(a) illustrates the effect of the shape of the cross section for the beams reinforced with steel reinforcement. The initial cracking load and ultimate load was 35 and 110 kN for square cross section. 32 and 100 kN was the initial and ultimate load for the circular cross section. 75 and 70 kN was the failure load for square and circular cross section. The initial cracking load and ultimate load for the square cross-sectional were higher than that of circular sections by 9% and 10%, respectively. The same results were recorded for the beams with steel wire mesh as illustrate in Figs. (b, c). The initial cracking load and ultimate load was 19 and 65 kN for square cross section. 18 and 60 kN was the initial and ultimate load for the circular cross section reinforced with welded steel wire mesh. 50.3 and 46.3 kN was the failure load for square and circular cross section reinforced with welded steel wire mesh. 16, 55 and 41.4 kN was the initial cracking, ultimate and failure load for the square cross section reinforced with expanded steel wire mesh while 15, 50 and 41.6 were being the initial cracking, ultimate and failure load respectively for the circular cross section reinforced with expanded steel wire mesh. The initial cracking load and ultimate load increased by 6% and 8%, respectively for the square cross-sectional compared with the circular cross sectional of the beam reinforced with welded steel wire meshes. Also; 7% and 10% increasing in the initial cracking load and ultimate load for the square cross sections compared with the circular cross section for the beams reinforced with expanded steel wire mesh.

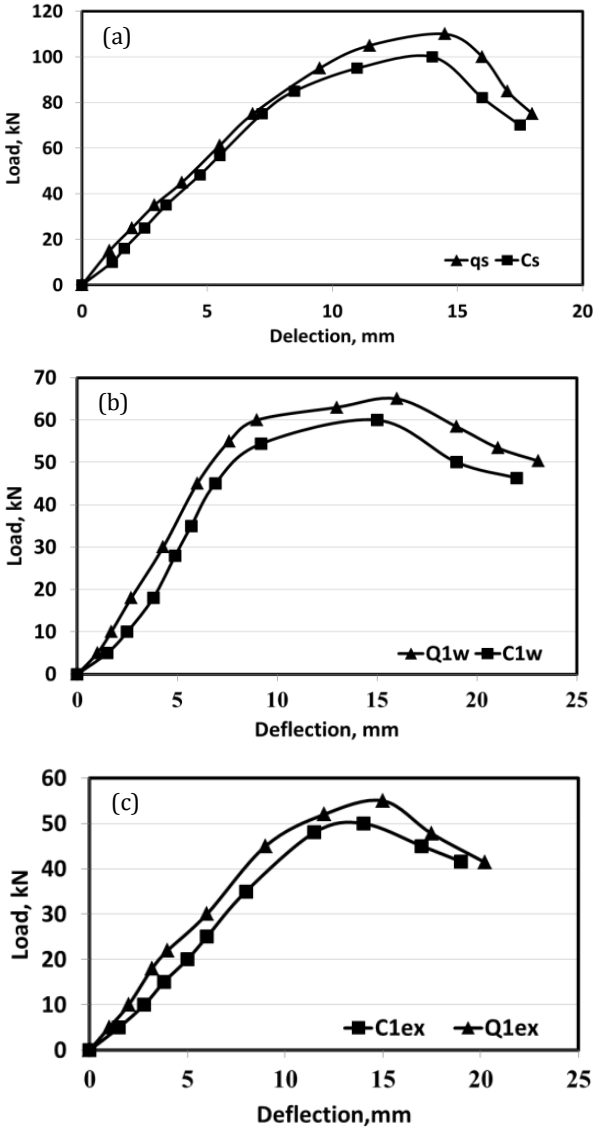

Fig. 4. Effect of shape of cross section: (a) Control specimens; (b) Specimens reinforced with welded wire mesh; (c) Specimens reinforced with expanded wire mesh.

6.2. Effect of number of mesh layers

The effect of numbers of steel wire mesh layer was shown in Figs. 5 and 6. As the number of steel wire mesh were increasing, the initial cracking, ultimate load and energy absorptions increase for all types of steel wire mesh and the shape of cross section.

For the beams with square cross sectional and reinforced with one layer welded steel wire mesh 19, 65 kN for initial and ultimate load. Also the energy absorption

was 1040 kN.mm. 22.8 and 80 kN were resulted for two layer in addition to 1500 kN.mm for energy absorption. The initial cracking load, ultimate load and energy absorption increased by 20%, 23% and 44% for the two mesh layers compared with one mesh layers, respectively. For the beams with circular cross sectional and reinforced with one layer welded steel wire mesh 18, 60 kN for initial and ultimate load. Also the energy absorption was 1190 kN.mm. 23.5 and 84 kN were resulted for two layer in addition to 1600 kN.mm for energy absorption. An increasing by 31%, 40% and 34% for the beam reinforced with two layer welded steel wire mesh compared with one layer welded steel wire mesh for with the circular cross sectional. For the beams with square cross sectional and reinforced with one layer expanded steel wire mesh, 16, 55 kN for initial and ultimate load. Also the energy absorption was 980 kN.mm. 23.3 and 70 kN were resulted for two layer in addition to 1150 kN.mm for energy absorption. The initial cracking load, ultimate load and energy absorption increased by 45%, 27% and 17% for the two mesh layers compared with one mesh layers, respectively. For the beams with circular cross sectional and reinforced with one layer expanded steel wire mesh 15, 50 kN for initial and ultimate load. Also the energy absorption was 1010 kN.mm. 21.4 and 75 kN were resulted for two layer in addition to 1210 kN.mm for energy absorption. An increasing by 43%, 50% and 20% for the beam with the circular cross sectional as illustrated in Fig. 6.

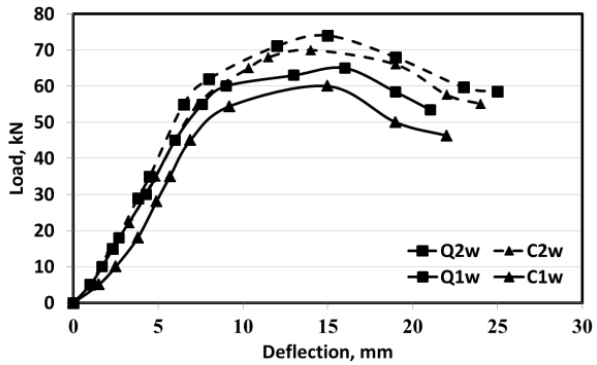

Fig. 5. Effect of number of layer for sections reinforced with welded wire mesh.

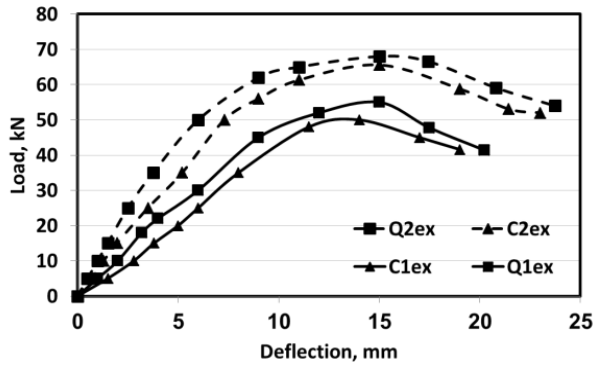

Fig. 6. Effect of number of layer for sections reinforced with expanded wire mesh.

6.3. Effect of type of reinforcement

Figs. 7 and 8 show the effect of types of reinforcement on the behavior of the tested beams with different of cross section. From these figures, the loads for conventional reinforcement were the highest compared with the two types of steel wire meshes. In addition to the loads for the beams reinforced with welded steel wire mesh are higher than that for beams reinforced with expanded steel wire mesh. However the energy absorption for the beams reinforces with steel wire meshes is higher than that reinforced with convention reinforcement. Fig. 7 illustrates the effect of type of reinforcement for square crass section. It is clear that; 35 and 110 kN were the initial cracking and ultimate load, respectively for the beam reinforced with conventional reinforcement. 19 and 22.8 kN was the initial cracking load for one layer and two layers welded steel wire mesh, respectively. The ultimate load was 65 and 80 kN for one layer and two layers respectively. For the square section with expanded wire mesh 16 and 23.3 kN was the initial cracking load for one layer and two layers expanded steel wire mesh, respectively. The ultimate load was 55 and 70 kN for one layer and two layers; respectively. A decreasing in the initial cracking and ultimate load by average 48 and 45% for welded and expanded steel wire meshes reinforcement compared with conventional reinforcement for the beams with square cross section. The increase in the initial cracking load was reduced to 33% for the two layers of reinforcement in both welded and expanded wire mesh. In addition to the increases in the ultimate load was reduce to 62% and 36% for welded and expanded wire mesh as illustrated in Fig. 7. On the opposed side the energy absorbed was decreased by 7 and 13% for the beams reinforced with one layers of welded and expanded steel wire meshes compared with conventional reinforcement as illustrated in Fig. 7. In addition to the energy absorption for the beams reinforced with two layers welded and expanded steel wire mesh increased by 33% and 2% compared with that conventional reinforced steel. An improvement in the initial cracking load and ultimate load by 15% for the one layers expanded wire mesh compared with one layer of welded steel wire. Also, an improvement in the initial cracking load and ultimate load by -3% and 12.5% for the two layers welded wire mesh compared with two layers of expended steel wire mesh. The same results were noticed for the beams with circular cross section as illustrated in Fig. 8. The initial cracking load, ultimate load and energy absorption were 18 kN, 60kN and 1190 kN.mm for one layer welded wire mesh. Also, 23.5 kN, 84 kN and 1600 kN.mm for initial cracking load, ultimate load and energy absorption for two welded steel wire mesh. The initial cracking load, ultimate load and energy absorption were 15 kN, 50kN and 1010 kN.mm for one layer expanded wire mesh. Also, 21.4 kN, 75kN and 1210 kN.mm for initial cracking load, ultimate load and energy absorption for two expanded steel wire mesh. A decreasing in the initial cracking and ultimate load by an average 48% and 45% for one layer of welded and expanded steel wire meshes reinforcement compared with the conventional reinforcement for the beams with circular

cross section. The energy absorbed was increased by 5% for the beams reinforced with one layers of welded steel wire meshes compared with conventional reinforcement. While a decreasing was noticed in the energy absorption by 2% for one layer expanded wire mesh compared with conventional reinforcement. The variation in the initial cracking load was reducing to 26% and 33% for two layers welded and expanded wire mesh compared with conventional reinforcement. Also the variation of ultimate load was reducing to 19% and 33% were for two layers welded and expanded wire mesh compared with conventional reinforcement. The energy absorbed was increased by 42% and 7% for the beams reinforced with two layers of welded and expanded steel wire meshes compared with conventional reinforcement. The initial cracking load, ultimate load and energy absorption was increases by 16%, 23% and 15% for one layer welded steel wire mesh compared with expanded steel wire mesh. Also, an improvement in the initial cracking load, ultimate load and energy absorption by 9%, 6% and 24% for the two layers of welded steel wire mesh compared with expanded steel wire mesh.

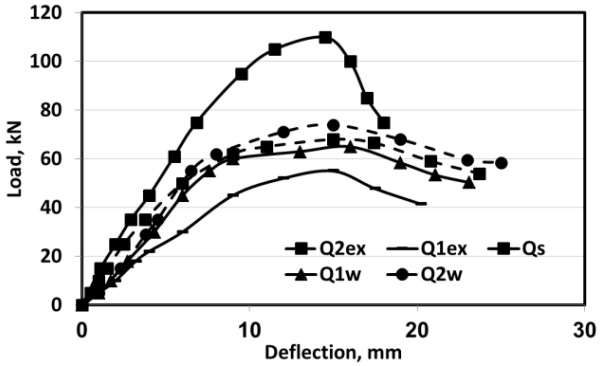

Fig. 7. Effect of types of reinforcement for square sections.

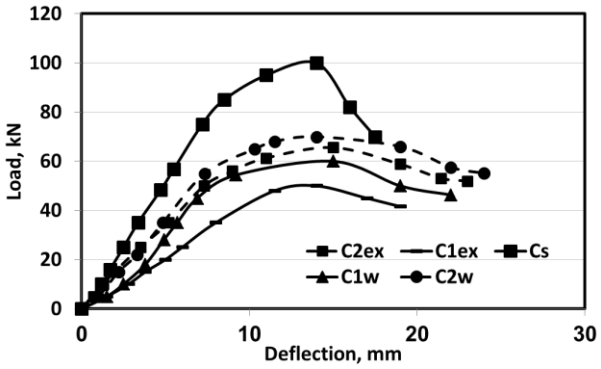

Fig. 8. Effect of types of reinforcement for square sections.

6.4. Effect of concrete cover

Fig. 9 shows the effect of concrete cover thickness for the beams with square cross section and reinforced with one layer welded steel wire mesh on the behavior of the tested beams. The initial cracking load, ultimate load and energy absorption was 19 kN, 65 kN and 1040 kN.mm, respectively for the specimen Q1w. While the initial cracking load, ultimate load and energy absorption was 18 kN, 67.5 kN and 1300 kN.mm respectively for specimens Q1wv. Decreasing the concrete cover thickness by 25% decreasing the initial cracking load by 5%; however increasing the ultimate load and energy absorption by 3.8% and 25%, respectively. For the beams with circular cross section, the initial cracking load, ultimate load and energy absorption was 18 kN, 60 kN and 1190 kN.mm, respectively for the specimen C1w. The initial cracking load, ultimate load and energy absorption was 16 kN, 62 kN and1400 kN.mm respectively for specimens C1wv. The initial cracking load decreased by 11%; however increasing the ultimate load and energy absorption by 3% and 17% respectively as illustrated in Fig. 10.

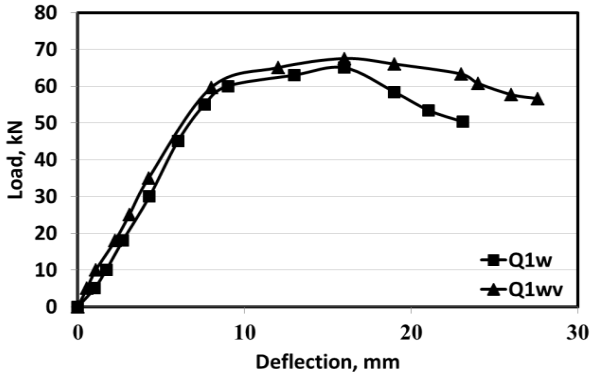

Fig. 9. Effect of concrete cover for square section.

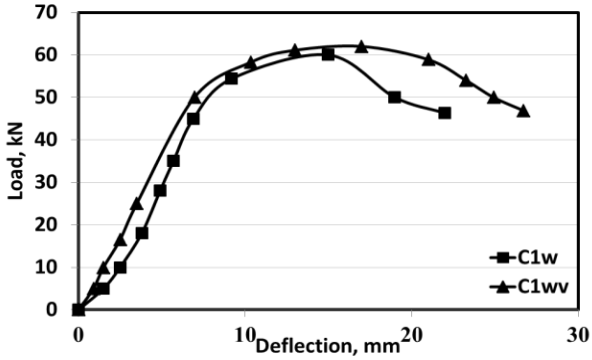

Fig. 10. Effect of concrete cover for circular section.

6.5. Effect of using steel bar as additional stirrups

The effect of using steel bar as additional stirrups on the behavior of the tested beams with one layer welded steel wire mesh was shown in Figs. 11 and 12. The use of stirrups resulted in the movement of the initial cracking load from the edges to the middle direction, in addition to delay the appearance of the initial cracking load. The initial cracking load, ultimate load and energy absorption was 19 kN, 65 kN and 1040 kN.mm, respectively for the specimen Q1w. While the initial cracking loads, ultimate load and energy absorption was 17.5 kN, 66 kN and 1430 kN.mm respectively for specimens Q1wr. The initial cracking load, ultimate load and energy absorption was 18 kN, 60 kN and 1190 kN.mm, respectively for the specimen C1w. While the initial cracking loads, ultimate

load and energy absorption was 15 kN, 61 kN and1480 kN.mm respectively for specimens C1wr. The initial cracking and ultimate load increased by -8% and 1.5% compared with the beams without stirrups for the tested beams with square and circular cross section. Also, the ratio of initial cracking load to ultimate load were 27% and 25% for the square and circular cross section the ratio of initial cracking load to ultimate load was changed by 2% and 5% for the square and circular cross section compared with the tested beams without steel stirrups.

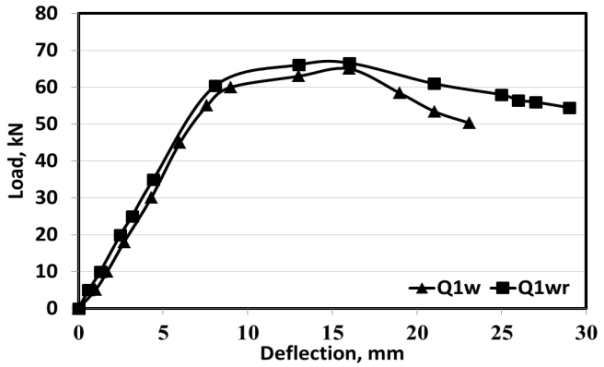

Fig. 11. Effect of using steel stirrups for square section.

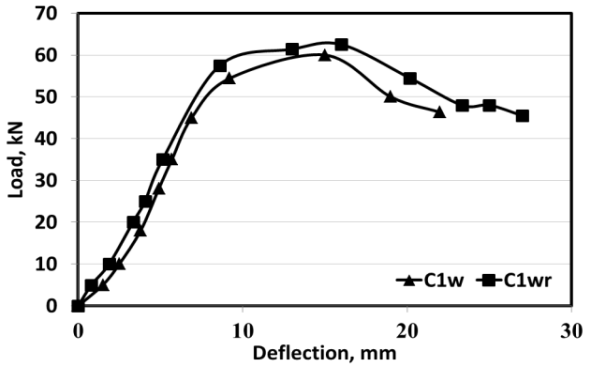

Fig. 12. Effect of using steel stirrups for circular section.

6.6. Ductility index and energy absorption

The test results are listed in Table 4. The table shows the obtained experimental results for each specimen as well as the ductility ratio, and energy absorption properties. Ductility ratio is defined here as the ratio between the mid-span deflections at ultimate load to that at the first crack load (Δ_u/Δ_y), while the energy absorption is defined as the area under the load-deflection curve. Computer program (BASIC language) was used to calculate the area under curve by integrated the equation of the load-deflection curve for each beam specimens as follow:

$$\text{Energy absorbed} = \int_0^{\Delta u} f(\Delta) d\Delta;$$

where: $f(\Delta)$ is the equation of load-deflection curve; Δ_u is the mid-span deflection at failure load.

The value of ductility index and energy absorption for all beams is presented in Table 4. It was observed the ductility behavior of circular hollow beams is better than of square beams. As the beams reinforced with wire meshes had ductility ratio more than with steel reinforcement due to the elongation of steel wire mesh is bigger than mild steel. The ductility ratio for the test specimens ranged from 3.0 to 4.06. The energy absorption of tested beams reinforced with steel wire meshes was higher than that with steel reinforcement due to increase the area under load deflection curve. Ductility index and energy absorption increased as the number of layers of steel wire meshes were increasing. This illustrates the effect of the stiffness of the beams.

6.7. Crack pattern

Cracking patterns for all the tested beams were illustrated in Fig. 13. All tested beams were un-cracked beam for the initial stages of loading. When the applied load reached to the rupture strength of the concrete on the specimen, the concrete started to crack up to the failure pattern in the all tested beams.

Table 4. Test results for the hollow beams.

Beam code	First crack load (kN)	Ultimate load (kN)	Deflection (mm)		Ductility index	Energy absorption (kN.mm)
			Δy	Δu		
Qs	35	110	4.7	15	3.14	1130
Cs	32	100	4.9	15.5	3.125	1000
Q1w	19	65	4.7	16	3.42	1040
C1w	18	60	4.2	14	3.33	1190
Q1ex	16	55	4.3	14.5	3.43	980
C1ex	15	50	4	13.5	3.33	1010
Q2w	22.8	74	3.3	11.5	3.5	1500
C2w	23.50	70	3.1	11	3.52	1600
Q2ex	23.30	68	4	12	3	1150
C2ex	21.40	65.5	3.6	12.5	3.5	1210
Q1wv	18	67.5	4	15	3.75	1300
C1wv	16	62	3.6	14	3.875	1400
Q1wr	17.50	66	3.55	13.5	3.77	1430
C1wr	15	61	3.7	15	4.06	1480

Fig. 13. Cracking pattern of tested beams.

7. Finite Element Model

A finite element package (ANSYS version 15), was used to simulate the behavior of hollow beams. Two types of elements were used; SOLID65 and LINK8. Fig. 14 shows the SOLID65 as 3-D reinforced concrete solid. Link 8 (Fig. 15) was defined by two nodes, the cross-sectional area, an initial strain, and the material properties. The steel wire meshes was defined by the volume fraction, initial strain and the material properties. Table 5 and Figs. 16 to 19 show some theoretical results for the ANSYS program.

Table 5. Comparison between theoretical and experimental results for first crack and ultimate loads.

Beam code	First crack load (kN)		Ultimate load (kN)	
	P_{theor}	$P_{exp.}/P_{theor}$	P_{theor}	$P_{exp.}/P_{theor}$
Qs	35	1.00	108	1.02
Cs	33	1.06	99	1.01
Q1w	20	0.95	65	1.00
C1w	19.5	0.92	62	0.97
Q1ex	15.5	1.03	55.5	0.99
C1ex	14	1.07	49	1.02
Q2w	22	1.04	78	0.95
C2w	25	0.94	72	0.97
Q2ex	24	1.04	70.7	0.96
C2ex	22	0.97	70.8	0.93
Q1wv	18	1.00	68.89	0.98
C1wv	15.8	1.01	62.6	0.99
Q1wr	17	1.03	64.68	1.02
C1wr	15.3	0.98	62.8	0.97
	Average = 1.003 S.D.= 0.0637		Average =0.98 S.D.= 0.0284	

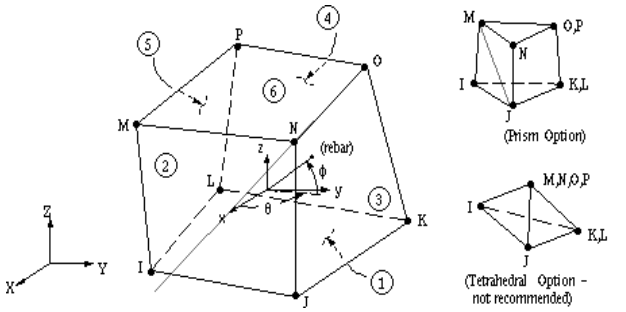

Fig. 14. SOLID65 3-D reinforced concrete solid.

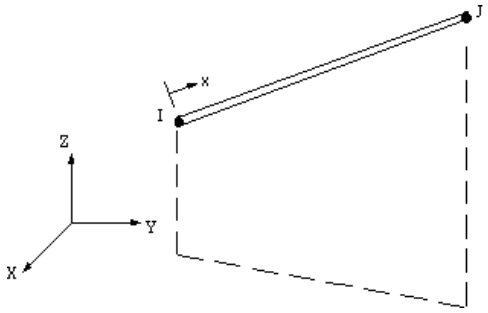

Fig. 15. LINK8 3-D spar.

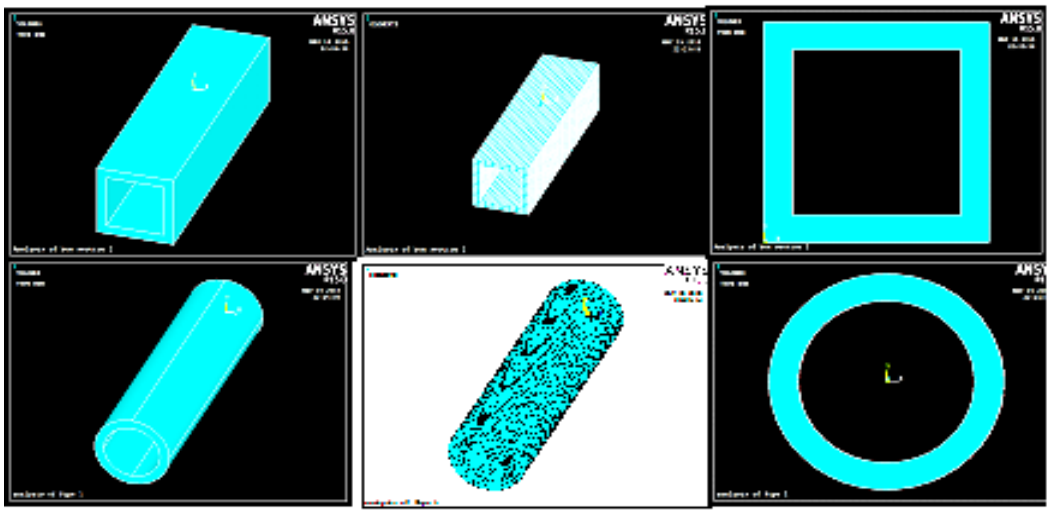

Fig. 16. Configuration of the tested hollow beams.

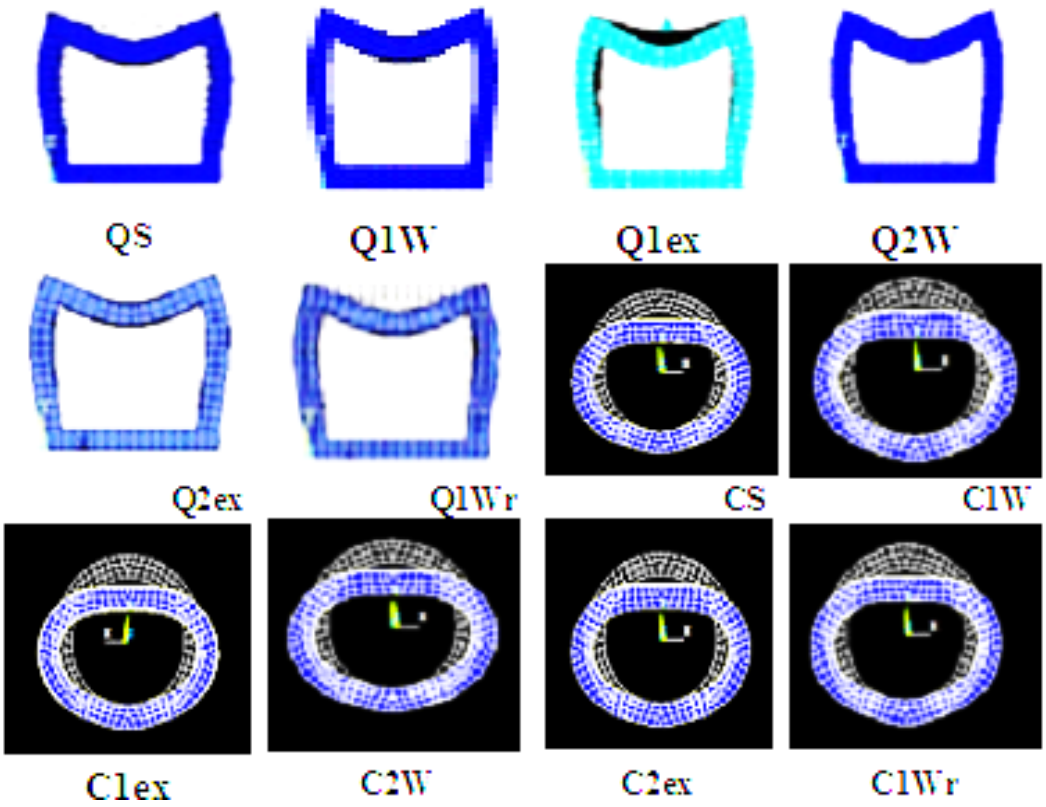

Fig. 17. Displacement of tested specimens.

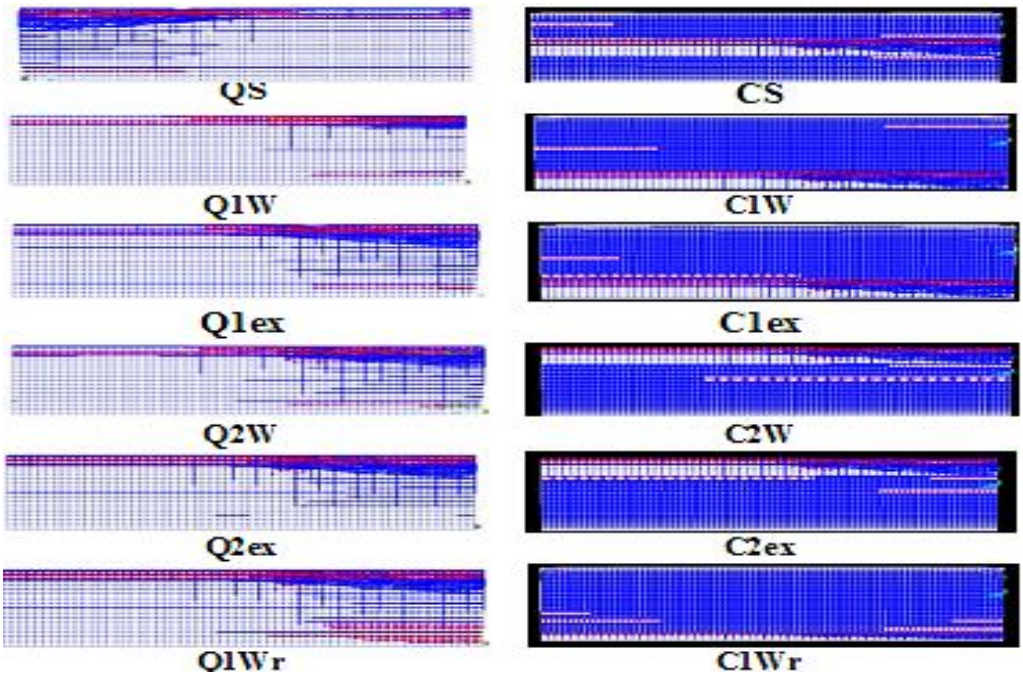

Fig. 18. Crack patterns of tested specimens.

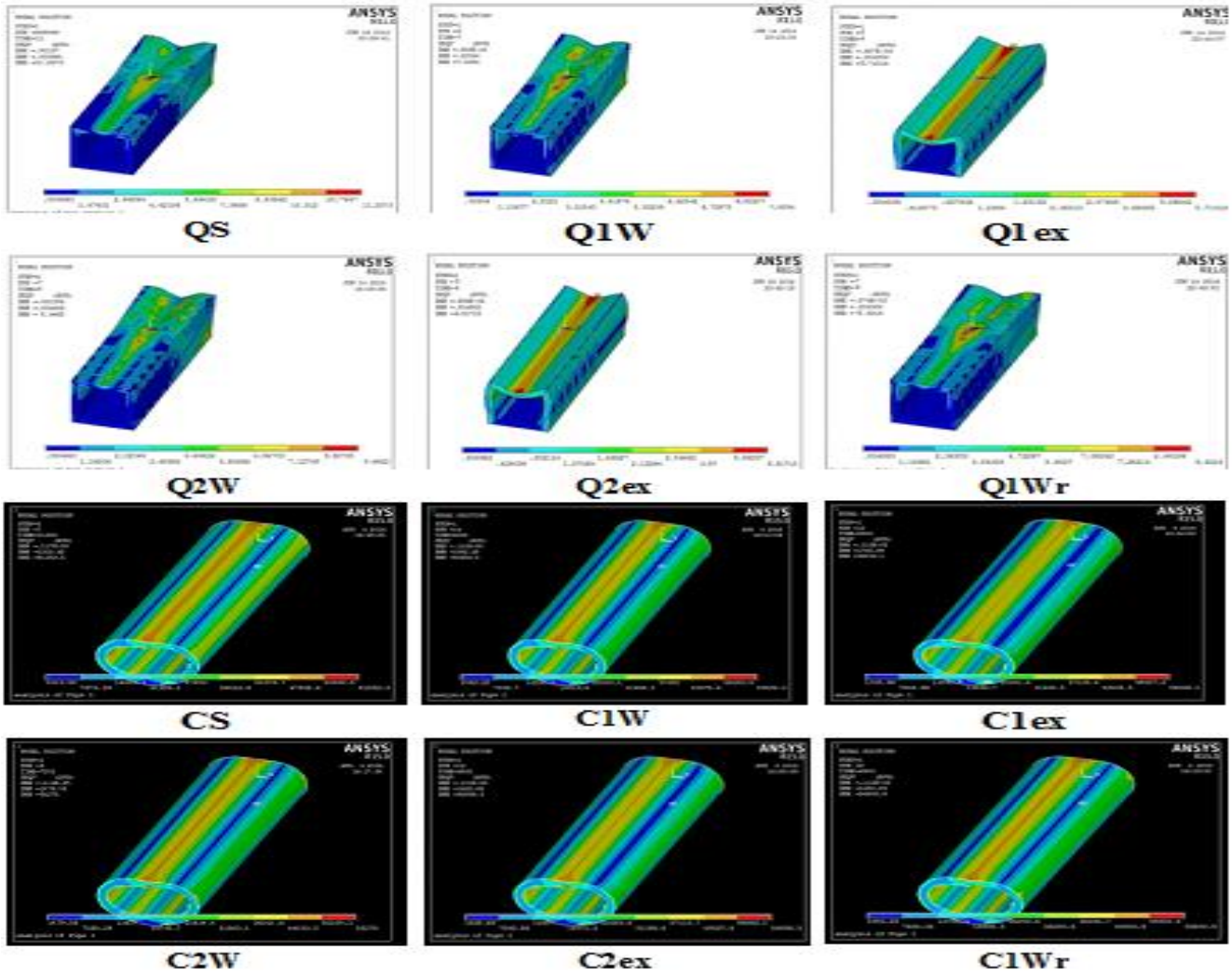

Fig. 19. Von Mises stress distribution for tested hollow beams.

8. Economic Assessment of Thin Section as Permanent Precast Units

As one of the applications, using self-compacted concrete, particularly in cast thin hollow sections. Theses sections cast as permanent precast units for construction tunnels. This way can offer save time in casting on the site and provide the cost of creating an alternate road. The cost comparison of thin hollow beam shown in Table 6. Tables 7 and 8 show the time-table for the conventional construction of the tunnel and the suggested method. Table 7 shows the stages of tunneling through traditional methods. This methods starting from digging the road which entails a leak and searching through an alternative to the work of converting it to traffic. It may require the expropriation of some land to increase the efficiency of the project. The preparing the chopping, wrenches, preparation for casting, and finally the tunnel ceiling not less than 18th week. Table 8 shows the time-table the proposed method for all the preparation, casting and post casting stages which are carried out in the factory away from the site. This method allows regular traffic without stopping at any time. Fig. 20 shows the main point of suggested method of installation of the pre-cast pieces in the site, which cast in the factory and quoted for the site. In suggested method, first step is digging the lane so that we can use the other parts of the lane. Moreover, we do not need to work alternative roads or cut off the road. The connection between the two pieces will connect only with the presence of a left lane for the road. When preparing for the third piece the right lane will open.

Table 6. Cost comparison of thin hollow beam.

code	Volume, m3	Concrete, kg/unit						Reinforcement						Total cost, L.E.
		cement	sand	Dolomite	Silica fume	HRWR	Cost	No. of layers	Area, m2	L.E./ m2	No. of bars	L.E./ bar	Length, m	
Qs	0.144	55	122	98	6	1.1	150	-	-	-	8	63	1.5	213
Cs	0.052	20	44.3	35.3	2	0.4	65							128
Q1w	0.096	36.8	81.8	65	4	0.74	86	1	2.4	16.8	-	-		102.5
C1w	0.038	15	32.4	25.8	1.6	0.3	40		1.875	13.125				53.125
Q1ex	0.096	36.8	81.8	65	4	0.74	86		2.4	16.8				119.6
C1ex	0.038	15	32.4	25.8	1.6	0.3	40		1.875	13.125				66.25
Q2w	0.096	36.8	81.8	65	4	0.74	86	2	4.8	33.6				119.6
C2w	0.038	15	32.4	25.8	1.6	0.3	40		3.75	26.25				66.25
Q2ex	0.096	36.8	81.8	65	4	0.74	86		4.8	33.6				119.6
C2ex	0.038	15	32.4	25.8	1.6	0.3	40		3.75	26.25				66.25
Q1wv	0.096	36.8	81.8	65	4	0.74	86	1	2.4	16.8	-	-		102.5
C1wv	0.038	15	32.4	25.8	1.6	0.3	40		1.875	13.125	-	-		53.125
Q1wr	0.096	36.8	81.8	65	4	0.74	86	1	2.4	16.8	2	20		122.8
C1wr	0.038	15	32.4	25.8	1.6	0.3	40		1.875	13.125				73.125

Note: The currency unit is the Egyptian pound (L.E), the date for the price calculation at January 2017.

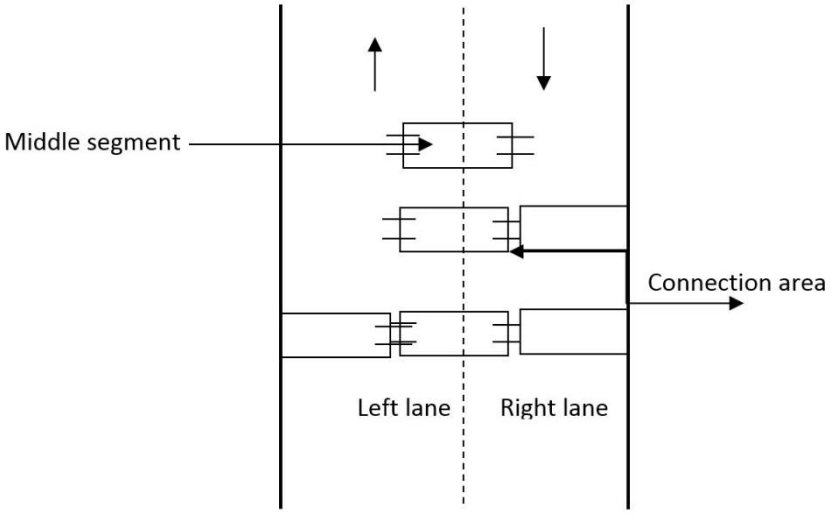

Fig. 20. Geometric shape for suggestion method.

Table 7. Time-table for conventional method.

code	1st week	2nd week	3rd week	4th week	5th week	6th week	7th week	8th week	9th week	10th week	11th week	12th week	13th week	14th week	15th week	16th week	17th week	18th week
Mobilization																		
Cutting asphalt																		
Excavation																		
Fixing floor form work																		
Fixing floor steel																		
Casting floor																		
Fixing walls form work																		
Fixing walls steel																		
Casting walls																		
Fixing roof scaffolding																		
Putting roof form work																		
Fixing roof steel																		
Casting roof																		
Removing scaffolding																		
Removing shuttering																		
curing																		
Painting inside tunnel																		
Fixing asphalt																		

Table 8. Time table for suggested method.

code	First week	2nd week	3rd week
Excavation +putting middle segment			
Right segment+casting overlap conection			
Left segment+casting overlap conection			
covering			

9. Conclusions

The following conclusions could be drawn from the results of the paper carried out to evaluate the behavior of thin hollow beams casting with self-compacting concrete:

- The initial cracking load for square cross section reinforced with conventional reinforcement, welded steel wire mesh and expanded steel wire mesh, increased by 9%, 6% and 7%, respectively compared with circular cross section.
- The ultimate load for square cross section reinforced with conventional reinforcement, welded steel wire mesh and expanded steel wire mesh, increased by 10%, 8% and 10%, respectively compared with circular cross section.
- Using welded steel wire mesh, the initial cracking load, ultimate load and energy absorption increased by 20%, 23% and 44% for the beam reinforced with two mesh layers compared with one mesh layers, respectively for square cross section. Also, the initial cracking load, ultimate load and energy absorption increased by 31%, 40% and 34%, respectively for the

beam reinforced with two layer steel wire mesh compared with one layer steel wire mesh for with the circular cross sectional.

- Using expanded steel wire mesh, the initial cracking load, ultimate load and energy absorption increased by 45%, 27% and 17% for the two layers compared with one mesh layers, respectively. Also, the initial cracking load, ultimate load and energy absorption increased by 43%, 50% and 20%, respectively for the beam reinforced with two layer steel wire mesh compared with one layer steel wire mesh for with the circular cross sectional
- A decreasing in the initial cracking and ultimate load by average 48 and 45% for one layer welded and expanded steel wire meshes reinforcement compared with conventional reinforcement for the beams with square and circular cross section.
- An increasing in the initial cracking load, ultimate load and energy absorption by 16%, 23% and 15% for circular cross sectional reinforced with one layer welded steel wire mesh compared with expanded steel wire mesh and by 9%, 6% and 24%, respectively for the two layers of welded steel wire mesh compared with expanded steel wire mesh.
- An improvement in the initial cracking load and ultimate load by 15% for the beam with square cross sectional reinforced with one layers expanded wire mesh compared with one layer of welded steel wire and by -3% and 12.5% for the two layers welded wire mesh compared with two layers of expended steel wire mesh.
- An increasing in the energy absorption by 5% for the beams reinforced with one layers of welded steel wire meshes compared with conventional reinforcement. While a decreasing was noticed in the energy absorption by 2% for one layer expanded wire mesh compared with conventional reinforcement.
- Using stirrups of mild steel bars with one layer welded wire mesh leads to increase the number of cracks and consequently increase the ultimate load by 1.5% in than that obtained when using only one layer without rings which lead to increase construction age. Moreover, the ratio of initial cracking load to ultimate load was 27% and 25% for the square and circular cross section, respectively.
- Decreasing the concrete cover thickness by 25%, the ultimate load and energy absorption increased by an average 3.8% and 25%, respectively for square cross section and 3% and 17% for circular cross section.
- Good agreement was found compared with the experimental results.
- Suggestion method in fixing precast tunnel cheaper and save time three times and six times respectively than ordinary method.
- These results clarify that there the increase in the ultimate load is 2.5% at slight increasing in the total cost.

REFERENCES

Abdel Hady SA (2003). Review article on self-compacting concrete. Zagazig University, Egypt.

ACI Committee 549 (2009). State-of-the-Art report on ferrocement. ACI549-R97, in manual of concrete practice. American Concrete Institute, Detroit.

ASTM C494/C494M (2001). Standard Specification for Chemical Admixtures for Concrete. Annual Book of ASTM Standards, 04, 02, 9.

Djamaluddin R, Bachtiar Y, Irmawati R (2014). Effect of the truss system to the flexural behavior of the external reinforced concrete beams. *International Journal of Civil, Architectural, Structural and Construction Engineering,* 8(6), 938-942.

E.S.S 4756-11 (2007). Physical and mechanical properties examination of cement, Part 1. Egyptian Standards Specification, Cairo.

Habib AM, Abelkrim L, Ammar Y (2016). Flowability and stability performance of self consolidating concrete in full-scale beam. *8th International RILEM Symposium on Self-Compacting Concrete*, 665-674.

Housing and Building Research Center (2002). State of the Art-Report on Self-Compacting Concrete. Strength of Material and Quality Control Department.

Khayat KH, Manai K, Trudel A (1997). In situ mechanical properties of wall elements cast using self-consolidating concrete. *ACI Materials Journal,* 94(6), 492-500.

Klug Y, Holschemacher K (2003). Material properties of hardened self-compacting concrete. http://aspdin.wifa.uni.-leipz[g.de/institute/lacer/lacer07/107_13.pdf

Kocher C, Watson W, Gomez M, Gonzalez I, Birman V (2002). Integrity of sandwich panels and beams with truss-reinforced cores. *Journal of Aerospace Engineering*, *ASCE,* 15(3), 111-117.

Manikandan S, Dharmar S, Robertravi S (2015). Experimental study on flexure behavior of reinforced concrete hollow sandwich beams. *P.S.R. Engineering College, International Journal*, 4, 45-60.

Olga R, Khanh N, Gonzalo B, Irene P, Mercedes G, Alberto S, R. Ángel R (2016). Assessment of pumpability quality control and performance parameters of SCC-type mixtures. *8th International RILEM Symposium on Self-Compacting Concrete,* 645-664.

Ouchi M (2000). Self-compacting Concrete Development, Applications and Investigations. http://www.is/ncr/publications/doc-23-3.pdf.

Ozawa K (1999). Proceeding of the International Workshop on Self-Compaction Concrete. Japan Society of Civil Engineers.

Pereira-de-Oliveira LA, Nepomuceno MCS, Castro-Gomes JP, Vila MFC (2014). Permeability properties of self-compacting concrete with coarse recycled aggregates. *Construction and Building Materials*, 51, 113-120.

Proske T, Graubner CA (2002). Self-Compacting Concrete-Pressure on Formwork and Ability to Deareat. *Ph.D. thesis*, Darmstadt.

Sara AS, Pedro R, Jorge B, Luis E (2017). Fresh state properties of self-compacting concrete with recycled aggregates - A literature review. *Athens Journal of Technology & Engineering*, March 2017, 33-46.

Shirai A, Ohama Y (1990). Improvement in flexural behavior and impact resistance of ferrocement by use of polymers. *Journal of Ferrocement,* 20(3), 247-264.

Skarendahi A (1998). Self-compacting concrete in Sweden. *Proceedings of International Symposium of Self-Compaction Concrete*, Kochi, Japan.

Vanhove Y, Djelal C, Magnin A, Martin D (2001). Study of self-compacting concrete pressure on formwork. Fukui: COMS Engineering Corporation. *Proceedings of the Second International Symposium on Self-Compacting Concrete*, Tokyo.

Yogendran V, Langan BW, Haque MN, Ward MA (1987). Silica fume in high strength concrete. *ACI Materials Journal*, 87-M51, 124-129.